THE JOURNAL OF BIOLOGICAL CHEMISTRY VOL. 289, NO. 3, pp. 1592–1603, January 17, 2014

Connexin43 Reduces Melanoma Growth within a Keratinocyte Microenvironment and during Tumorigenesis *in Vivo*[*]

Received for publication, August 1, 2013, and in revised form, December 2, 2013 Published, JBC Papers in Press, December 2, 2013, DOI 10.1074/jbc.M113.507228

Mark J. Ableser[‡], Silvia Penuela[‡], Jack Lee[§], Qing Shao[‡], and Dale W. Laird[‡§1]

From the Departments of [‡]Anatomy and Cell Biology and [§]Physiology and Pharmacology, The University of Western Ontario, London, Ontario N6A 5C1, Canada

Background: Cx43 is a gap junction protein that is highly expressed in the epidermis.
Results: Ectopic expression of Cx43 in gap junctional intercellular communication-deficient melanomas reduces growth in keratinocyte co-cultures and tumorigenicity assays.
Conclusion: Cx43 acts as a tumor suppressor during melanoma tumorigenesis.
Significance: Cx43 may serve as a potential therapeutic target for melanomas.

Connexins (Cx) have been identified as tumor suppressors or enhancers, a distinction that appears to be dependent on the type and stage of disease. However, the role of connexins in melanoma tumorigenesis and their status during cancer onset and progression remain controversial and unclear. Here, we show that the aggressive B16-BL6 mouse melanoma cell line expresses low basal levels of Cx26 and Cx43, rendering them gap junctional intercellular communication-deficient as elucidated by immunofluorescence, Western blotting, and dye transfer studies. Following ectopic expression of green fluorescent protein-tagged Cx26 and Cx43 in these connexin-deficient melanomas, punctate gap junction-like plaques were evident at sites of cell-cell apposition, and the incidence of dye transfer was significantly increased similar to connexin-rich keratinocytes. We found that the expression of Cx43, but not Cx26, significantly reduced cellular proliferation and anchorage-independent growth from control melanomas, whereas migration was unaffected. Additionally, melanomas expressing Cx43 displayed significantly reduced growth within the *in situ*-like microenvironment of keratinocytes, despite a lack of heterocellular gap junctional intercellular communication between the two cell types. Furthermore, when grown *in vivo* in the chicken chorioallantoic membrane, primary tumors derived from Cx43-expressing melanomas were significantly smaller than controls, whereas Cx26-expressing melanomas produced tumors similar to controls. Collectively, these results suggest that Cx43, and not Cx26, can act as a tumor suppressor during melanoma tumorigenesis.

Connexins (Cx)[2] are a family of integral membrane proteins that can oligomerize into hexamers, known as connexons, and dock with connexons from apposing cells forming gap junction channels (1). The gap junction-mediated exchange of small molecules (<1 kDa) between cells is known as gap junctional intercellular communication (GJIC), and this process is critical for the maintenance of cellular homeostasis and regulation of controlled cellular events including proliferation, differentiation, and apoptosis (1). Although it is commonly accepted that the primary function of connexins is to assemble into gap junctions to allow for GJIC, connexons also possess the ability to act as single-membrane hemichannels, allowing for the exchange of signaling molecules with the extracellular environment (2). The human genome encodes 21 distinct connexins, which are expressed in some combination in virtually all cell types of the body (1). Interestingly, as many as 10 connexins, including Cx26 and Cx43, are expressed in human epidermis with a similar subset expressed in rodent epidermis (3). Primarily, these connexins are expressed by keratinocytes and are differentially regulated within the different epidermal strata (3). Additionally, melanocytes, which reside in the basal layer of the epidermis, have been reported to only express Cx26 and Cx43 (4, 5). Typically, one melanocyte forms contacts with ~30 keratinocytes within the basal and suprabasal layers forming the "epidermal-melanin unit" (6), and the connexin compatibilities of the two cell types render them capable of heterocellular GJIC (4). It has been suggested that melanocyte growth is regulated by keratinocytes through GJIC (6) as well as the exchange of other regulatory signals (7–9).

Gap junctions were first implicated as being important in tumorigenesis nearly 50 years ago (10). Since then, many investigators have reported that connexins are down-regulated or even absent in cancer cell lines, resulting in compromised GJIC (10–14) and, furthermore, observed reductions in tumorigenic behaviors when connexins were ectopically reintroduced into tumor cells (15–19). These findings, combined with the observations that Cx32 knock-out mice are more prone to developing chemical- and radiation-induced tumors (20, 21), support the notion that connexins have tumor suppressor properties. However, more recently, connexins have been shown to facilitate tumor progression and metastasis in late stage disease, leading to their reclassification as "conditional tumor suppres-

* This work was supported by funds from the Canadian Institutes of Health Research (to D. W. L.).
[1] To whom correspondence should be addressed: Dept. of Anatomy and Cell Biology, The University of Western Ontario, Dental Science Bldg. 00077, London, ON N6A 5C1, Canada. Tel.: 519-661-2111, Ext. 86827; Fax: 519-850-2562; E-mail: dale.laird@schulich.uwo.ca.
[2] The abbreviations used are: Cx, connexin; GJIC, gap junctional intercellular communication; REK, rat epidermal keratinocytes; EdU, 5-ethynyl-2′-deoxyuridine; CAM, chorioallantoic membrane; MEM, minimal essential medium.

sors" (22). Given this paradox, it is not surprising to find that the role of connexins during the onset and progression of melanoma tumorigenesis is controversial and remains poorly understood. Although the majority of research suggests that melanomas exhibit poor GJIC because of connexin deficiencies (4, 23–25), recent research suggests that connexins may be facilitators of late stage disease (23, 26, 27), alluding to a potential biphasic role of connexins during melanoma tumorigenesis.

When studying tumorigenesis, it is important to consider the *in situ* tumor cell microenvironment to account for contact-dependent and diffusible factors that may influence tumor growth and progression. In particular, when studying the role of connexins in tumorigenesis, the *in situ* microenvironment takes on further importance because direct cell to cell contact is needed to facilitate GJIC. In the case of melanoma, the loss of the ability to form heterocellular contacts and exhibit GJIC with keratinocytes may be a contributor to melanoma growth within the epidermis (4, 28), whereas GJIC between melanomas and fibroblasts or endothelial cells may enhance tumor progression and metastasis (23, 26, 27). Thus, it is imperative to study connexins during melanoma tumorigenesis in a multidimensional context that encompasses *in situ* and *in vivo* environments to better understand how tumor cells behave during cancer progression while also in the setting of normal cell types.

Using this approach, we sought to further assess the role of connexins and GJIC during melanoma tumorigenesis in a unifying model mindful of the melanoma microenvironment. We found that the metastatic B16-BL6 mouse melanoma cell line (BL6) expressed only low basal levels of Cx26 and Cx43, rendering them GJIC-deficient. Following ectopic expression of both connexins, we established GJIC among melanoma cells, but this failed to restore GJIC with keratinocytes. The expression of Cx43 in melanomas significantly reduced proliferation and anchorage-independent growth *in vitro*, reduced growth within the *in situ*-like microenvironment of keratinocytes, and reduced primary tumor size within the *in vivo* microenvironment of the chicken embryo. Conversely, the expression of Cx26 did not affect the aggressive behavior and tumorigenic properties of melanomas. Taken together, these studies strongly suggest that Cx43, but not Cx26, is capable of suppressing melanoma tumorigenesis.

EXPERIMENTAL PROCEDURES

Cell Culture—The murine melanoma cell line B16-BL6 (kindly provided by Dr. Moulay Alaoui-Jamali, McGill University) was cultured in minimal essential medium (MEM) containing 2 mM L-glutamine, 10% FBS, 100 units/ml penicillin, 100 μg/ml streptomycin, 0.1 mM MEM nonessential amino acids, MEM vitamin solution, and 1 mM MEM sodium pyruvate (Invitrogen). Rat epidermal keratinocytes (REK, kindly provided by Dr. Vincent Hascall, Cleveland Clinic Lerner Research Institute) were cultured in DMEM with 4.5 g/liter glucose 1× supplemented with 2 mM L-glutamine, 10% FBS, 100 units/ml penicillin, and 100 μg/ml streptomycin (Invitrogen). All cells were incubated at 37 °C and 5.0% CO_2.

Generation of Melanoma Cell Lines—BL6 cells were stably infected with an empty AP2 replication-defective vector or vectors encoding Cx43-GFP or Cx26-GFP as previously described (29). Newly engineered Cx26-GFP and Cx43-GFP expressing cells were plated at very low density in 10-cm dishes and allowed to grow into isolated colonies for 2 weeks. Using an inverted epifluorescence microscope (Leica Microsystems), isolated colonies enriched in GFP expression were identified and subsequently picked and allowed to expand in 12-well plates. Of the isolated colonies selected, the Cx26- and Cx43-expressing colonies that were most enriched in GFP expression were determined and used for the remainder of the experiments.

Immunocytochemistry and Western Blotting—Control and connexin overexpressing melanomas were cultured on coverslips, grown to confluence, and fixed in 10% neutral buffered formalin. Fixed cells were blocked and permeabilized with 3% BSA, 0.1% Triton X-100 in PBS for 1 h and immunolabeled with rabbit anti-Cx26 (1:200 dilution; Invitrogen, 51-2800), rabbit anti-Cx43 (1:500 dilution; Sigma), mouse anti-N-cadherin (1:200 dilution; BD Transduction Laboratories), and/or mouse anti-E-cadherin (1:500; BD Transduction Laboratories) antibodies for 1 h at room temperature, followed by washes and incubation with Alexa Fluor® 488-conjugated anti-rabbit (1:500 dilution; Molecular Probes) or Alexa Fluor® 555-conjugated anti-mouse (1:1,000 dilution; Molecular Probes) secondary antibodies. Nuclei were stained with Hoechst 33342 dye prior to mounting on glass slides with Airvol.

In the case of Western blotting, protein lysates were collected from confluent monolayers (or over-confluent cultures of REKs to assess for Cx26) in a lysis buffer (1% Triton X-100, 150 mM NaCl, 10 mM Tris/HCl, pH 7.4, 1 mM EDTA, 1 mM EGTA, and 0.5% Nonidet P40, supplemented with protease inhibitor mixture (Roche Applied Sciences) and phosphatase inhibitors (1 mM sodium fluoride and 1 mM sodium orthovanadate)). Protein concentrations were determined using a BCA (bicinchoninic acid) protein determination kit (Pierce). Total protein lysates (35 or 50 μg) were resolved by SDS/PAGE and transferred onto nitrocellulose membranes using the iBlot Dry Blotting System (Invitrogen). Membranes were blocked using 5% Blotto, nonfat dry milk (Santa Cruz) for 1 h before being immunolabeled with rabbit anti-Cx26 (1:1,000 dilution; Invitrogen, 71-0500), rabbit anti-Cx43 (1:5,000 dilution; Sigma), mouse anti-GFP (1:7,500 dilution; Millipore), or mouse anti-β-tubulin (1:7,500 dilution; Sigma) antibodies at 4 °C. Primary antibodies were detected using the fluorescently conjugated anti-rabbit Alexa Fluor® 680 (1:10,000 dilution; LI-COR Biosciences) or anti-mouse IRdye 800 (1:10,000 dilution; LI-COR Biosciences) antibodies and scanned using the Odyssey Infrared Imaging System (LI-COR Biosciences).

Microinjection—Cells grown to confluence were microinjected with 10 mM Alexa Fluor® 350 hydrazide (Molecular Probes), which is known to permeate through gap junctions (30), using an Eppendorf Femojet automated pressure microinjector. Images were collected using a Leica DM IRE2 inverted epifluorescence microscope equipped with Openlab 5.5.3 imaging software. The percentage of cells that passed dye to at least one neighboring cell was recorded. For each biological replicate, 15 injections were performed on each cell line, and statistical analysis was performed on the average of three biological replicates.

Growth Curve and Proliferation—Cells were plated into individual wells of a 6-well plate at a density of 1×10^4 cells/well. On days 2, 4, 5, and 6, cells were lifted from the plate with 500 μl of 0.25% trypsin-EDTA (Invitrogen) and counted using a Countess automated cell counter (Invitrogen) or supplemented with fresh medium. Statistical analysis was performed on the average of two technical replicates of four biological replicates. In parallel, cells were plated on coverslips at a density of 1×10^4 cells/well. On day 4, cells were incubated with fresh medium containing 1 μg/ml 5-ethynyl-2′-deoxyuridine (EdU) for 3 h and subsequently fixed in 3.7% formalin for 15 min at room temperature. Cells were labeled using the Click-It® EdU Alexa Fluor® 488 cell proliferation kit (Molecular Probes) according to the manufacturer's instructions. The fluorescence of GFP within the engineered cells was quenched because of the intensity of the fluorescence from the conjugated Alexa Fluor® 488 azide. As such, to visualize the presence of GFP, cells were counterstained with a mouse anti-GFP (1:500 dilution, Millipore) antibody followed by an Alexa Fluor® 555-conjugated anti-mouse (1:1,000 dilution, Molecular Probes) antibody. Images were collected using a Leica DM IRE2 inverted epifluorescence microscope equipped with Openlab 5.5.3 imaging software. For each biological replicate, 10 blinded, randomized images were taken using the 63× lens, and the percentage of EdU-positive cells compared with total nuclei was counted using ImageJ 1.46r (National Institutes of Health). Statistical analysis was performed on the average of four biological replicates.

Anchorage-independent Growth—BL6 cells were plated at a density of 1×10^4 cells/well in 0.3% soft agar suspension atop a polymerized 0.4% soft agar layer. For each biological replicate, BL6 cells were plated in six wells for each treatment. Cultures were grown for 10 days under normal conditions. Images were collected using a Leica DM IRE2 inverted epifluorescence microscope and Openlab 5.5.3 imaging software. For each well, 10 randomized images were taken with a 5× lens. Colonies that were greater than 50 μm in diameter were counted, and the average number of colonies/mm^2 was determined. Statistical analysis was performed on the average of four biological replicates.

Migration Scrape Assay—Control and engineered BL6 cells were plated on etched grid plates and grown to confluence prior to treating with 25 μg/ml Mitomycin C (Sigma) for 30 min in normal medium. The cells were scraped along a straight line down the midline of the grid plate with a rubber cell scrapper, clearing half the plate of cells. Cells were then supplemented with serum-free MEM. Five intersecting grid points were marked along the scrape edge as reference points. Images were collected using a Leica DM IRE2 inverted epifluorescence microscope equipped with Openlab 5.5.3 imaging software. Images were taken at each reference point at 0, 24, and 48 h using a 5× lens. For each reference point, the distance from the scrape edge (0 h) to the leading migratory edge (24 and 48 h) was measured using ImageJ 1.46r (National Institutes of Health). Statistical analysis was performed on the average of four biological replicates.

Co-culture Melanoma Growth—REKs were plated at a density of 5×10^4 cells/well and co-cultured with BL6 cells at a density of 1×10^4 cell/well. Mixed cell cultures were supplemented with DMEM and MEM at a 4:1 ratio, respectively, and were grown for 6 days to confluence. Clusters were identified under phase contrast because of their morphological differences, and their melanoma phenotype was confirmed by the presence of GFP-tagged connexins in engineered cells. For each biological replicate, 10 blinded, randomized images were taken using a 5× lens. Under phase contrast, melanoma clusters were outlined using ImageJ 1.46r (National Institutes of Health), and the total area of all melanoma clusters for a given field was determined. Statistical analysis was performed on the average area occupied by BL6 cells of four biological replicates.

Co-culture Microinjections—REKs were co-cultured with BL6 cells at a 10:1 ratio, respectively. Mixed cell cultures were supplemented with DMEM and MEM at a 4:1 ratio, respectively, and allowed to grow to confluence. Melanoma clusters were identified under phase contrast because of their morphological differences, which were confirmed by the presence of GFP-tagged connexins in engineered cells. BL6 cells or REKs at the melanoma-keratinocyte boundary were microinjected with 10 nM Alexa Fluor® 350 hydrazide (Molecular Probes) using an Eppendorf Femojet automated pressure microinjector. Images were collected using a Leica DM IRE2 inverted epifluorescence microscope equipped with Openlab 5.5.3 imaging software. The percentage of injected BL6 cells that passed dye to at least one neighboring BL6 or REK was recorded. Similarly, the percentage of injected REKs that passed dye to at least one neighboring REK or BL6 was recorded. For each biological replicate, at least six REKs and six BL6 cells were injected. Statistical analysis was not performed because of a complete lack of heterocellular dye transfer between different cell types over three biological replicates.

In Vivo Chick Chorioallantoic Membrane (CAM) Assay—Primary tumor properties of BL6 cells in the chicken embryo was assessed as previously described (31). Briefly, fertilized chicken eggs (McKinley Hatchery, St. Mary's, Canada) were incubated in an automated rotary incubator (GQF Manufacturing Company) under 40% humidity at 37 °C for 3 days, rotating once every hour. Eggs were removed from their shell and placed in covered dishes. Chicken embryos were incubated for an additional 7 days in stationary incubators (GQF Manufacturing Company) under 60% humidity at 37 °C. On day 11 of development, 3.0×10^5 control or connexin-expressing BL6 cells in 20 μl of serum-free MEM were topically applied to a site of major branching vessels on the CAM distal to the embryo and covered with a coverslip. The embryos were returned to a humidified 37 °C stationary incubator for 7 days to allow tumor growth. Primary melanoma tumors that formed at the site of topical application were excised, weighed, and imaged. Statistical analysis was performed on the primary tumor weights of 18 control and 15 Cx43-GFP- and 11 Cx26-GFP-expressing melanoma tumors.

Statistics—Statistical analysis was performed on all results using a one-way analysis of variance followed by a Tukey's post hoc test in which $p < 0.05$ was considered significant. The values are presented as means ± S.E. In the case of primary tumor weights, each data point represents an isolated tumor from individual embryos, and statistical analysis was performed on

the mean tumor weight between each experimental group. All statistics were performed using GraphPad Prism Version 4.03 for Windows.

RESULTS

Expression of Cx26 and Cx43 Increases Gap Junctions and GJIC in Mouse Melanoma Cells—The mouse melanoma cell line BL6 expressed low levels of both Cx26 and Cx43 as indicated by immunofluorescence (Fig. 1*A*) and Western blot analysis (Fig. 1, *B* and *C*). Cx26 was observed only in over-confluent REKs, whereas Cx43 was readily detectable in these cells (Fig. 1*A*, *insets*). Following ectopic expression of Cx26-GFP and Cx43-GFP, BL6 cells exhibited punctate gap junction-like structures that localized to the cell surface as indicated by their co-localization with the cell adhesion molecule N-cadherin (Fig. 1*A*, *arrows*). Western blots revealed the low levels of Cx26 and Cx43 in BL6 cells compared with REKs, whereas both Cx26-GFP and Cx43-GFP were readily detected upon their ectopic expression (Fig. 1, *B* and *C*). Additionally, both fusion proteins displayed similar expression levels when probed for GFP (Fig. 1*D*).

To assess the GJIC capacity of control and engineered cells, all cell lines were microinjected with the small molecular dye Alexa350, and the incidence of dye transfer to neighboring cells was measured. Wild-type and vector control BL6 cells were found to be GJIC-deficient only passing dye from ~25% of the microinjected cells (Fig. 2*A*, *arrows*). Conversely, Cx26-GFP- and Cx43-GFP-expressing melanomas displayed significantly increased dye transfer, resulting in 80 and 100% of the microinjected cells passing dye to neighboring cells, respectively ($p < 0.05$). The Cx26 and Cx43 engineered cells acquired a GJIC status that was statistically similar to Cx43-rich and well coupled REKs (Fig. 2*B*). Thus, our findings show that both Cx26 and Cx43 are able to establish functional GJIC in BL6 cells.

Cx43 Expression in Melanomas Significantly Reduces Cell Proliferation—When subjected to a 6-day growth curve analysis, Cx43-expressing BL6 cells displayed a significantly reduced total cell number compared with controls as early as day 4 ($p < 0.05$), which was further amplified on days 5 and 6 (2.5-fold; $p < 0.001$). Conversely, Cx26 did not impart as profound an effect on total cell number, but there was a slight reduction of ~20% in cell number on day 6 ($p < 0.05$) (Fig. 3*A*).

To determine whether the effect of Cx43 on total cell numbers was due to changes in cell proliferation, we used an EdU labeling assay at day 4 to determine the number of cells actively cycling through the S phase. Using unsynchronized cells, EdU was able to incorporate into cells undergoing S phase during a 3-h incubation period. We found that the expression of Cx43 in BL6 cells significantly reduced the percentage of EdU+ cells by ~25% from controls ($p < 0.01$) (Fig. 3, *B* and *C*). Consistent with our growth curve analysis, the expression of Cx26 did not significantly reduce the percentage of EdU+ cells (Fig. 3*C*). Collectively, Cx43 was found to decrease total cell numbers by reducing the rate at which cells pass through the S phase of the cell cycle.

Cx43-expressing Melanomas Display a Less Pronounced Malignant Phenotype—When grown in soft agar suspension to assess for anchorage-independent growth, the amount of colonies formed from Cx43-expressing melanomas was significantly reduced by ~4.5-fold from controls ($p < 0.001$). Conversely, the expression of Cx26 in BL6 cells did not significantly reduce anchorage-independent growth (Fig. 4, *A* and *B*). Using a scrape assay, the migratory distance from the wound edge at 0 h (Fig. 4*C*, *left panel*, *red line*) to the leading edge at 48 h (Fig. 4*C*, *right panel*, *red line*) was not statistically different between control and Cx-expressing melanomas (Fig. 4*D*).

Cx43 Expression in Melanomas Reduces Growth in an in Situ-like Microenvironment Independent of Heterocellular GJIC with Keratinocytes—BL6 cells were co-cultured at a low density with REKs and allowed to grow to confluence over 6 days. Identifiable BL6 cell clusters were observed under phase contrast (Fig. 5*A*, *left column*, *dashed lines*), and their melanoma phenotype was confirmed because of the expression of GFP-tagged connexins within the outlined areas in engineered cells. Wild-type and control melanomas were found to occupy ~14% of the two-dimensional field of view. Melanomas expressing Cx26 did not grow as robustly as control melanomas in the context of the keratinocytes and were found to occupy slightly less area, but this was not statistically significant. The expression of Cx43, however, significantly reduced the total area occupied by melanoma clusters by ~4.5-fold compared with controls ($p < 0.05$) (Fig. 5, *A* and *B*).

Using this co-culture model, we assessed for heterocellular GJIC between melanomas and keratinocytes by microinjecting both cell types at the melanoma-keratinocyte interface. Again, when BL6 cells were co-cultured with Cx-rich REKs, identifiable melanoma clusters were observed under phase contrast, similar to before (Fig. 6, *left column*, *dashed lines*). As expected, connexin-deficient melanomas were poorly coupled to each other and did not transfer Alexa350 dye to the Cx43-rich keratinocytes. Although connexin-expressing melanomas displayed high incidence of dye transfer with neighboring melanoma cells, in all cases, they failed to pass dye to adjacent keratinocytes. Similarly, when keratinocytes were injected at the melanoma-keratinocyte border, REKs were highly coupled with neighboring REKs but never transferred dye to adjacent melanoma cells, regardless of connexin status (Fig. 6).

Because of the lack of heterocellular dye transfer between melanomas and keratinocytes, connexin localization was assessed at the melanoma-keratinocyte interface. Keratinocytes express an abundance of Cx43, which readily assembled into gap junctional plaques and regionally expressed Cx26 upon their stratification and differentiation in culture. Despite the expression of both connexins in REKs, gap junctional plaques were not readily evident at REK/melanoma interfaces even when BL6 cells were engineered to express Cx43-GFP or Cx26-GFP (Fig. 7). Occasionally, Cx43 staining was apparent at potential heterocellular interfaces, but given the rarity of these findings and the lack of heterocellular gap junction dye transfer, we suggest that these locations represent sites of REK homocellular processes.

Cx43-expressing Melanomas Display Reduced Primary Tumor Size in Vivo—Using the *in vivo* chicken embryo model, control or connexin-expressing melanomas were topically applied to 10-day-old embryos and allowed to grow for 1 week. In all cases, primary tumors formed at the sight of topical application (Fig.

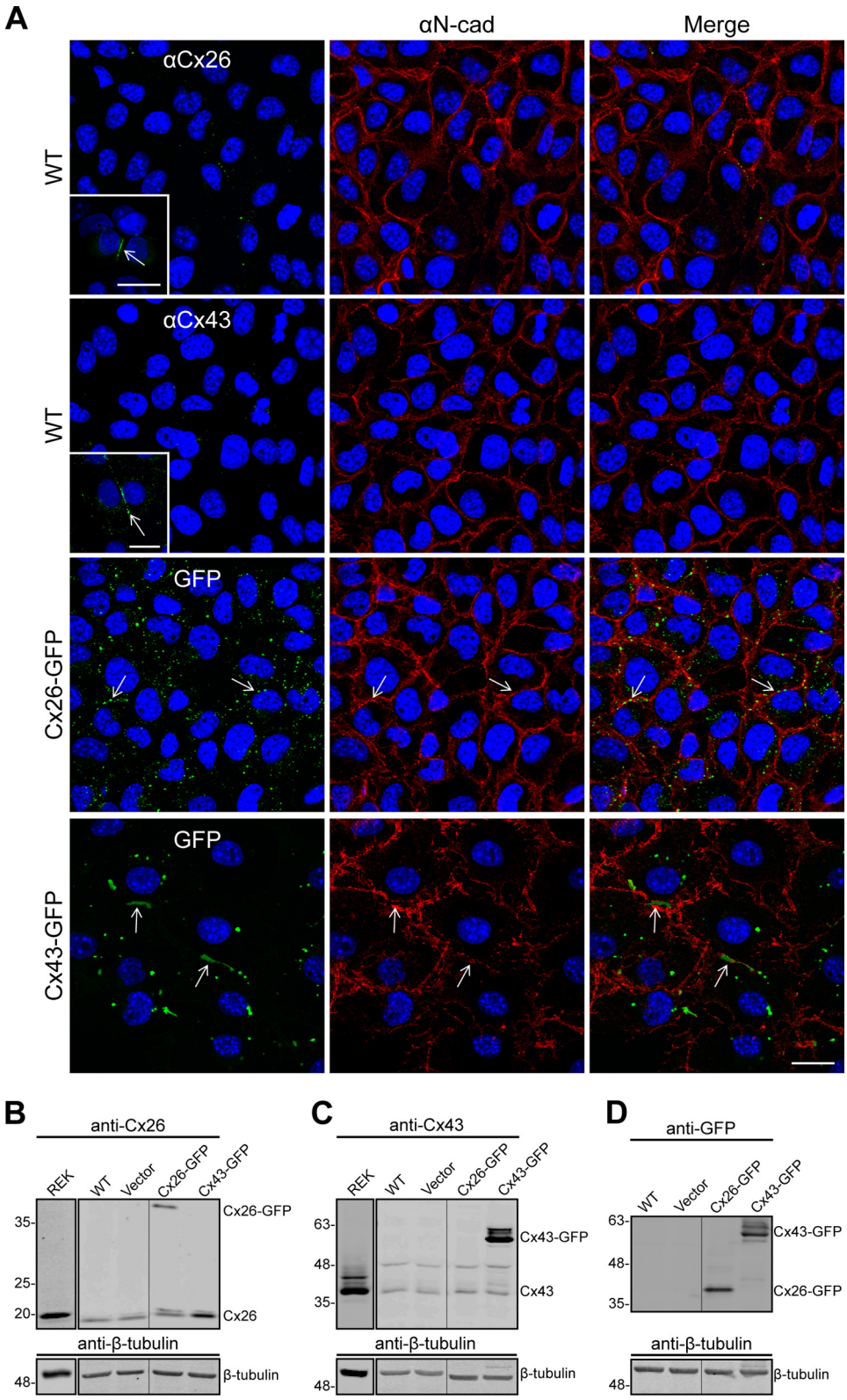

FIGURE 1. **BL6 mouse melanomas express low levels of Cx26 and Cx43.** *A*, immunofluorescence revealed that WT BL6 cells endogenously express low levels of Cx26 and Cx43 compared with REKs, which display typical gap junctional plaques at sites of cell-cell apposition (*inserts*). *B* and *C*, Western blots confirmed the low levels of Cx26 and Cx43 in melanomas compared with lysates collected from over-confluent and confluent REK cultures, respectively. Following ectopic expression of Cx26-GFP or Cx43-GFP, punctate gap junction-like plaques were evident at the cell surface as denoted by the cell adhesion molecule N-cadherin (*red*) (*A, arrows*), and the expression of GFP-tagged connexins was readily detected by Western blots immunolabeled for Cx26 (*B*) or Cx43 (*C*). *D*, additionally, both fusion proteins were expressed at similar levels as detected by Western blots immunolabeled for GFP. β-Tubulin was used as a loading control. The vector control represents cells transfected with a construct that did not encode connexins. *Lanes* separated by *vertical lines* were run on the same blot but spliced together. *Lanes* loaded with REK lysates were run as independent experiments. *Blue*, nuclei; *bars*, 20 μm.

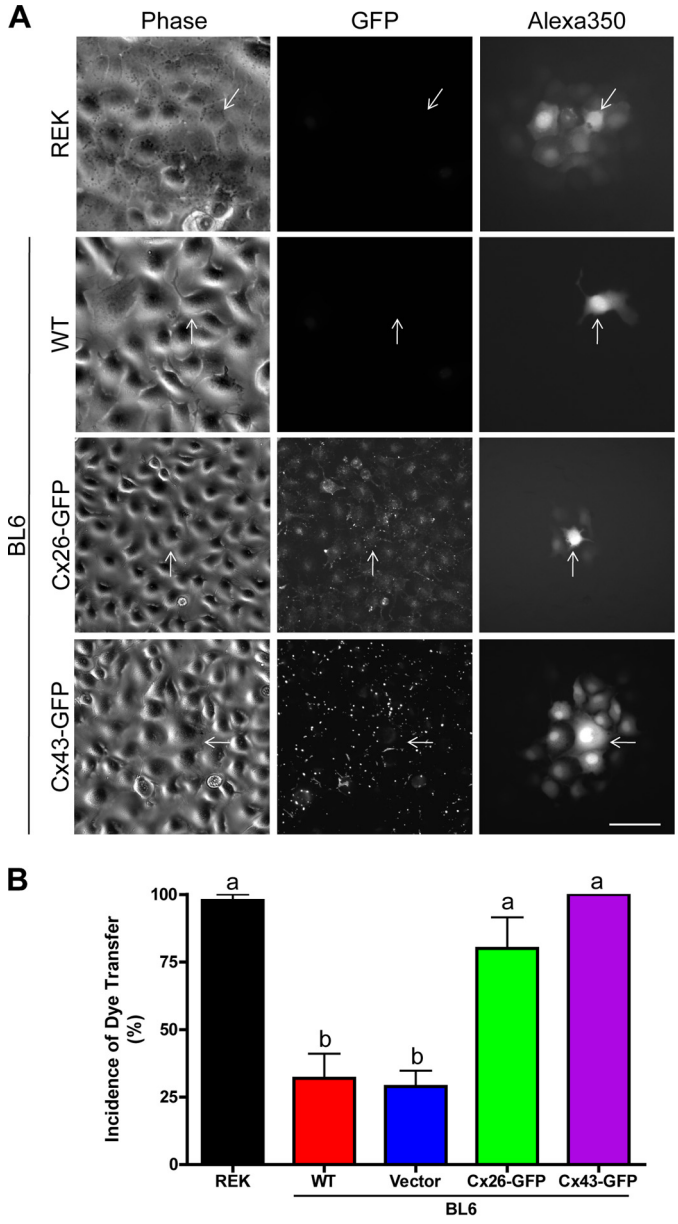

FIGURE 2. **Ectopic connexin expression significantly increases GJIC.** *A*, Alexa350 dye transfer studies revealed that wild-type and control melanomas were poorly coupled, because dye rarely spread from the microinjected cell (*arrows*) to neighboring cells. *B*, following ectopic expression of Cx26-GFP or Cx43-GFP, the incidence of dye transfer was significantly increased to 80 and 100%, respectively, statistically similar to Cx43-rich REK controls ($n = 45$, $p < 0.05$). Phase contrast images depict cellular morphology prior to microinjection, whereas the GFP fluorescence denotes the expression of ectopic connexins. *Letters* depict statistical significance among the groups. *Bar*, 40 μm.

8*A*, *arrows*). Primary tumors were excised, and excess CAM was removed from the tumor mass. Embryos inoculated with control melanomas produced large, blood engorged tumors averaging ~0.09 g in weight. The expression of Cx26 within these tumors did not significantly reduce primary tumor weights in the chick CAM assay. Conversely, Cx43-expressing melanomas exhibited significantly reduced primary tumor weight, producing tumors averaging ~0.02 g, which represents a reduction in tumor mass of ~4.5-fold compared with the vector control ($p < 0.001$) (Fig. 8, *A* and *B*). These tumors appeared more diffuse, less blood-filled, and occasionally less pigmented. Together, these studies suggest that Cx43 is a potent tumor suppressor in melanomas in the *in situ*-like microenvironment of keratinocytes as well as *in vivo*.

DISCUSSION

The role of connexins in melanoma tumorigenesis remains poorly understood because some studies support the notion that connexins behave as tumor suppressors, whereas other reports suggest that connexins in melanomas facilitate the spread of the disease during metastasis (4, 23–27). Although the connexin family is large, most evidence suggests that the two prominent connexins in melanocytes are Cx26 and Cx43, which enables GJIC with keratinocytes (4, 5). This direct cell to cell communication is often lost during melanoma transformation, which appears to be due to connexin down-regulation (4, 23). Most studies pertaining to connexins in melanomas tend to focus on specific stages of tumorigenesis; however, in no studies have connexins been studied in a unifying model system where connexin-expressing melanoma cells are evaluated *in vitro*, within the context of keratinocytes and *in vivo*. Here, we show that Cx43, and not Cx26, is an effective tumor suppressor in melanomas that reside in the context of keratinocytes and *in vivo*.

In the present study, we chose to ectopically express GFP-tagged Cx26 and Cx43 in an aggressive, gap junction-deficient BL6 mouse melanoma cell line. Previously, we and others have shown that the GFP tag exhibited negligible changes to the function and localization of both these connexins (32–37). As expected, both connexins readily assembled into gap junctions and established extensive functional GJIC as assessed by dye transfer assays. In our study, we examined the incidence of dye transfer and not the degree of dye spread, because of the intrinsic differences between the two connexins in question. Cx26 channels are expected to be more restrictive in the passage of transjunctional molecules in comparison to Cx43 channels because of their predicted smaller pore size (38). Regardless, both connexins were shown to significantly increase dye transfer, similar to connexin-rich keratinocytes.

Because connexins have been defined as conditional tumor suppressors (22), it is possible that their effects on cell characteristics associated with tumorigenesis may vary in early and late stage disease, as has been suggested to occur in melanomas (23). Many connexin family members have been reported to inhibit cell proliferation in several cancer cell types (15, 39). To that end, ectopic expression of Cx43 has been shown to reduce cell proliferation in many distinct cancers (17, 40, 41). Here, we show that Cx43 expression in Cx-deficient melanomas reduces the total cell number via delayed passage through the S phase of the cell cycle. Likewise, the expression of Cx26 in cancer cells has also been reported to reduce cell proliferation (34), as has the related and often co-expressed Cx30 isoform (42). However, here we found that Cx26 exhibited no significant effect on cell proliferation in melanomas, suggesting tumor cell specific differences. Mechanistically, it has been suggested that Cx43 reduces proliferation in glioblastomas by inhibiting cell cycle progression through GJIC-independent mechanisms (40). These findings are consistent with later studies where Cx43 was suggested to control cell cycle progression at the G_1 phase

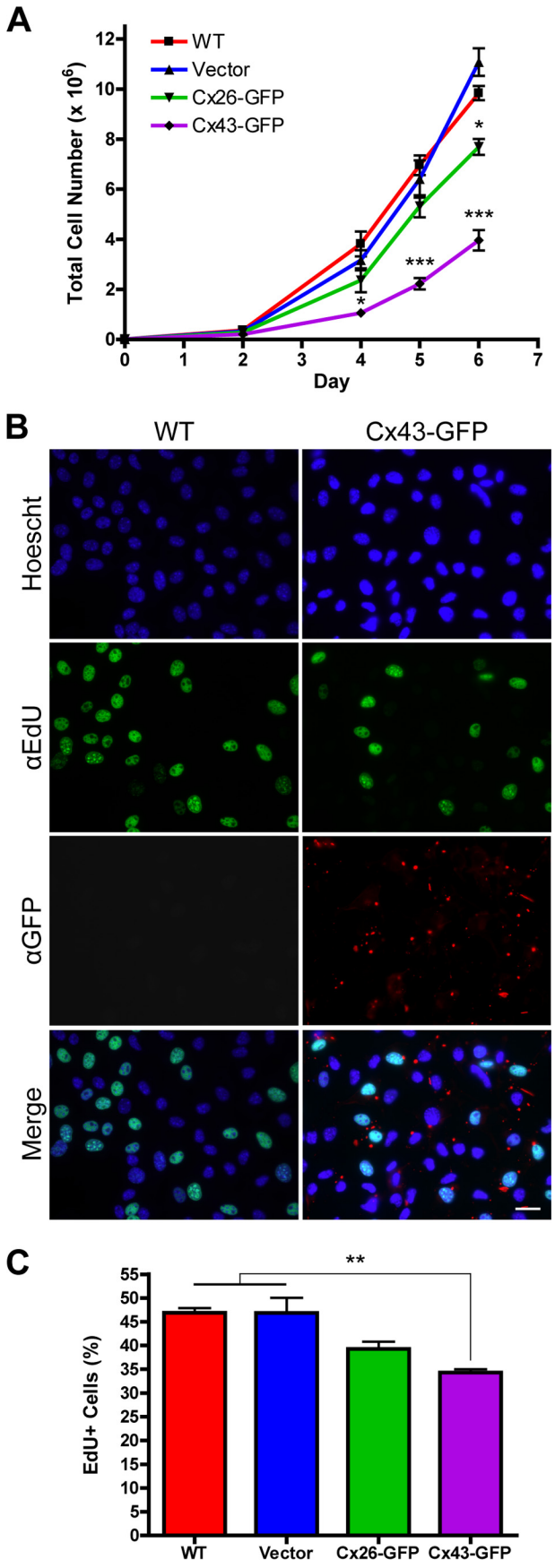

FIGURE 3. **Expression of Cx43 significantly reduces total cell number and cell proliferation.** *A*, 6-day growth curves revealed that Cx43-GFP-expressing melanomas displayed significantly reduced total cell number as early as day 4 ($n = 8$; *, $p < 0.05$), which was further reduced on days 5 and 6 ($n = 8$; ***, $p < 0.001$). Cx26-GFP-expressing melanomas displayed a slight reduction in total cell number only on day 6 ($n = 8$, *, $p < 0.05$). *B*, proliferation at day 4 was assessed using an EdU assay, which labels nuclei passing through the S phase of the cell cycle, where the proportion of EdU-labeled nuclei (*green*) to total nuclei labeled with Hoescht (*blue*) was determined. Cells were counterstained with an anti-GFP antibody (*red*) because the normal fluorescence of GFP-tagged Cx43 was quenched by the EdU signal. *C*, expression of Cx43 significantly reduced the percentage of EdU-positive cells by ~25% in comparison to the controls ($n = 40$; **, $p < 0.01$). *Bar*, 20 μm.

through increased expression of p27, a cyclin-dependent kinase inhibitor, as a result of the inhibition of the S phase kinase-associated protein, Skp 2 (43). Additionally, Cx43 has also been reported to decrease the expression of several cyclins and cyclin-dependent kinases in transformed kidney epithelium (44), although the necessity of channel function was not assessed.

Cx26 has been shown to reduce anchorage-independent growth in several cancer cell types (16, 45), as has Cx43 (16, 24, 40). Importantly, Cx43 has been reported to reduce anchorage-independent growth in melanomas (24) similar to our results, whereas Cx26 was not previously assessed. Interestingly, Omori and Yamasaki (45) showed that in HeLa cells, C-terminally truncated Cx43 was capable of establishing GJIC and also reducing anchorage-independent growth. Thus, passage of molecules through intercellular channels or hemichannels is likely causing the cellular changes rather than binding of one of the many members of the interactome that have been reported to bind to the C terminus of Cx43 (46).

In some tumor cell types, connexins have also been reported to affect migration. For example, Cx26, but not Cx43, has been shown to reduce migration in breast tumor cells (34). Similarly, Zucker *et al.* (47) reported that both wild-type Cx43 and a channel-dead Cx43 mutant did not alter migration in melanoma cells. Although Cx26 and Cx43 do not consistently play a role in melanoma cell migration, as our *in vitro* studies show, one must also consider the many factors of the *in vivo* microenvironment because connexins have been shown to be up-regulated and correlated to increased melanoma metastasis (23, 26, 27). However, this complex process encompasses other cellular events, in addition to migration, in which connexins have been deemed important, including extravasation (48, 49).

In the epidermis, the growth and homeostasis of melanocytes (the precursors to melanomas) are regulated by epidermal keratinocytes, which together with melanocytes form the epidermal-melanin unit (4, 6, 7). Heterocellular GJIC is established between keratinocytes and melanocytes for the putative passage of regulatory signals that coordinate the epidermal-melanin unit (4). As expected, connexin-deficient melanomas that arise are not only isolated from each other but also from keratinocytes, as we discovered in mixed cell cultures of these two cell types. Somewhat to our surprise, connexin-expressing melanomas also remained functionally isolated from keratinocytes, despite the ability of both cell types to express either Cx26 or Cx43. Their lack of ability to re-establish heterocellular GJIC may be due to the cadherin differences between melanomas and keratinocytes, expressing N-cadherin and E-cadherin, respectively, as previously reported (4). In support of this con-

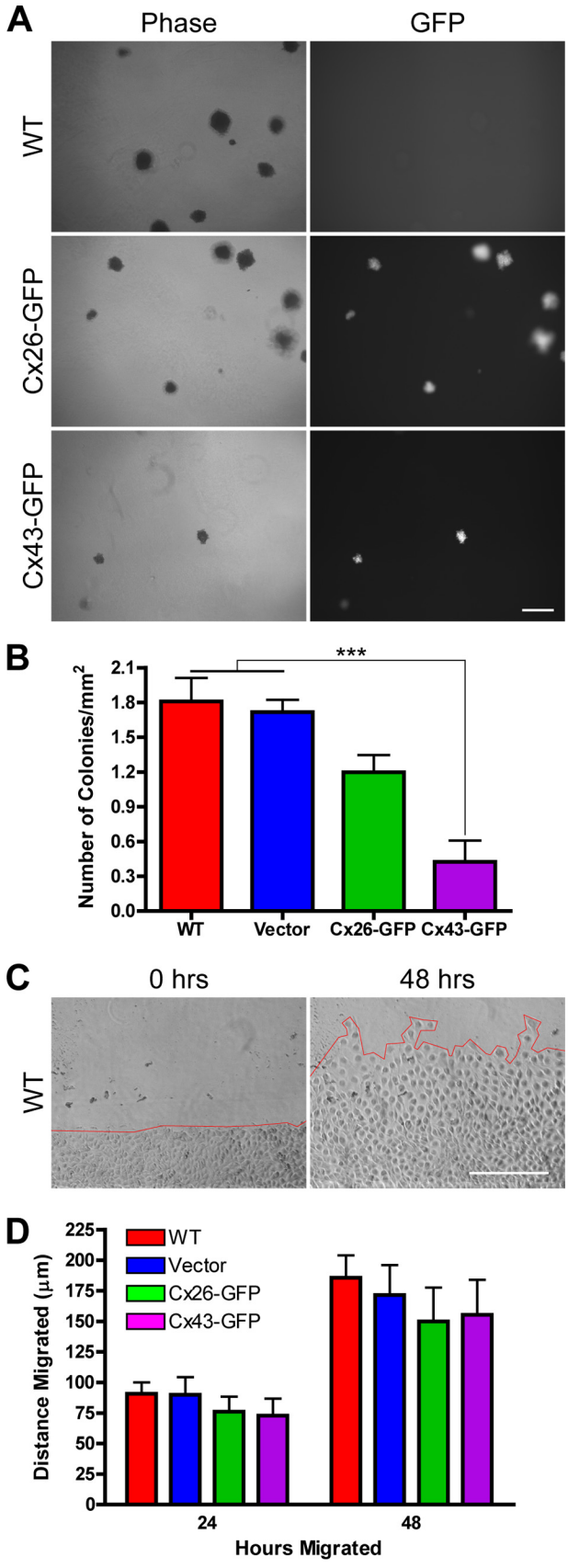

FIGURE 4. **Cx43 expression significantly reduces anchorage-independent growth, whereas cell migration remains unaffected.** *A*, when grown in soft agar suspension for 10 days, cell colonies were evident under phase contrast, and those formed from Cx-expressing melanomas were GFP-positive. *B*, the number of colonies formed was significantly reduced in melanomas expressing Cx43-GFP by ~4.5-fold in comparison to controls ($n = 240$; ***, $p < 0.001$), whereas Cx26-GFP expression did not significantly alter the number of cell colonies ($n = 240$, $p =$ ns). *C*, using a scratch assay, the migratory ability of Cx-deficient and Cx-expressing melanomas was assessed. Cells were grown to confluence, pulsed with 25 μg/ml of Mitomycin C for 30 min, scratched (*red line at 0 h*), and supplemented with serum-free medium. *D*, the distance migrated from the initial scratch edge to the leading edge after 24 and 48 h (*C*, *red line* at *48 h*) was not statistically different between Cx-deficient and Cx-expressing melanomas ($n = 20$, $p =$ ns). *Bars*, 200 μm.

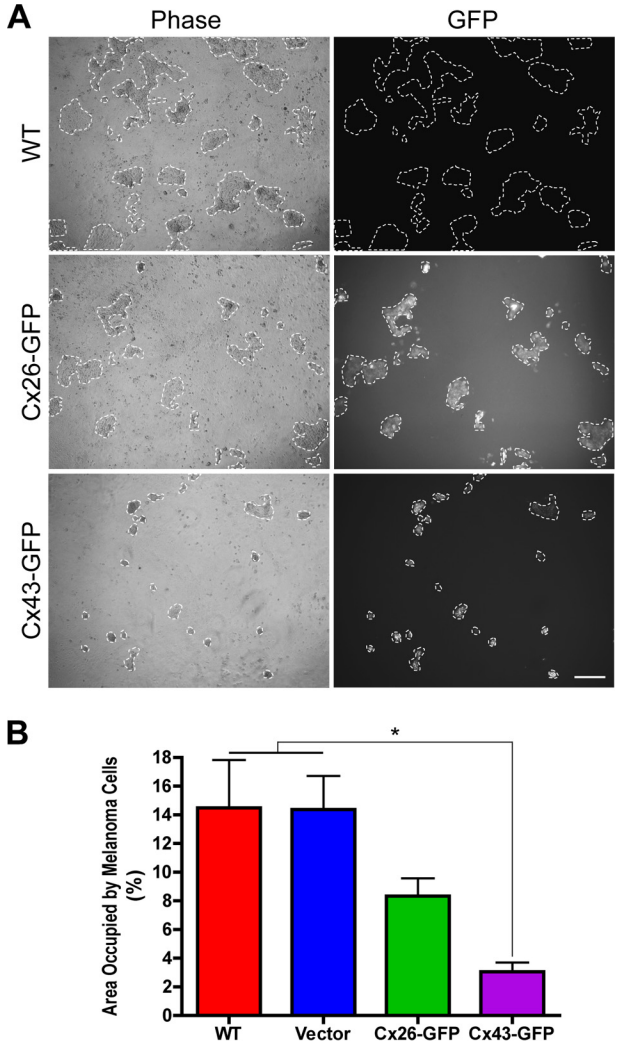

FIGURE 5. **Expression of Cx43 significantly reduces melanoma growth within a keratinocyte-based microenvironment.** *A*, melanomas were co-cultured with keratinocytes at a 1:5 ratio and allowed to grow for 6 days. Under phase contrast imaging, melanoma clusters were identifiable (*dashed lines*), and their melanoma phenotype was confirmed in engineered cell lines because of the expression of GFP. *B*, the area of all melanoma clusters for a given field was measured, and Cx43-expressing melanomas were found to occupy ~4.5-fold less area than controls ($n = 40$; *, $p < 0.05$). *Bar*, 200 μm.

cept, it has been reported that melanomas that retained E-cadherin expression, as well as melanomas that were engineered to express E-cadherin, could establish GJIC with keratinocytes (4), producing a less malignant phenotype (28). In contrast to this, we show that increasing Cx43-based GJIC between melanomas can significantly inhibit melanoma cell growth when grown in the microenvironment of keratinocytes, despite not re-establishing heterocellular GJIC with keratinocytes. This inhibition of growth in co-culture was significantly higher than the mod-

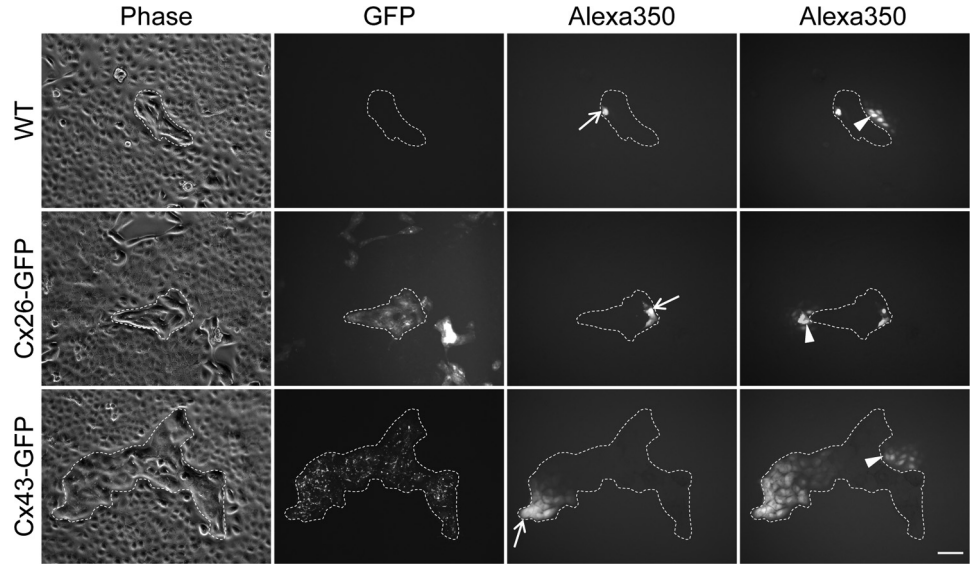

FIGURE 6. **Ectopic connexin expression in melanomas does not establish heterocellular GJIC with keratinocytes.** Melanomas were co-cultured with keratinocytes at a 1:10 ratio, respectively. Under phase contrast, melanoma clusters were identified (*dashed lines*), and their melanoma phenotypes were confirmed, where possible, by the expression of GFP. In all cases, injected melanomas (*arrows*) failed to pass Alexa350 to adjacent keratinocytes, and only Cx-expressing melanomas exhibited sufficient dye transfer among each other ($n = 18$). Similarly, keratinocytes injected with Alexa350 (*arrowheads*) were highly coupled with neighboring keratinocytes, but in all cases, failed to pass dye to adjacent melanomas ($n = 18$). *Bar*, 50 μm.

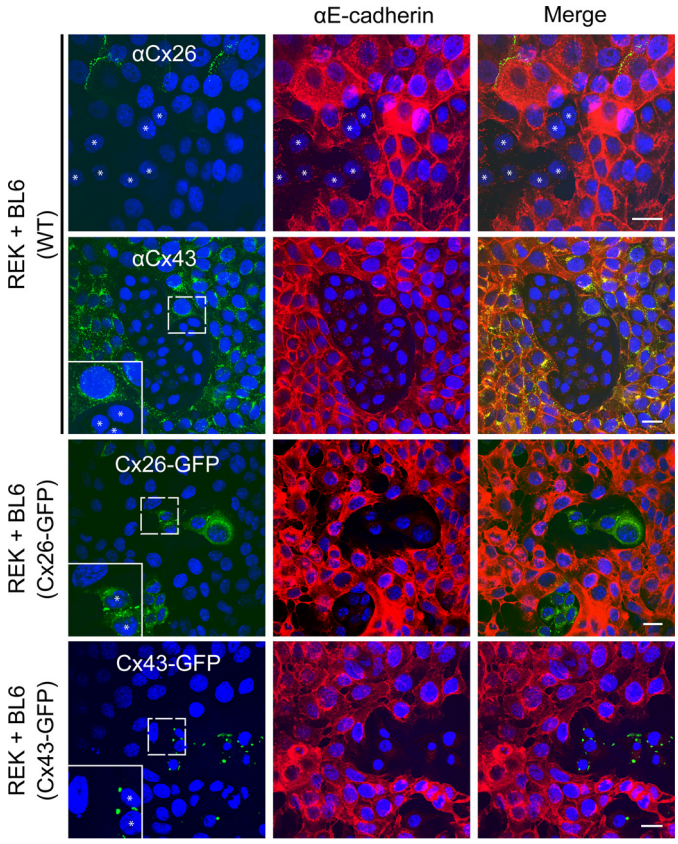

FIGURE 7. **Cx26 or Cx43 do not act to form melanoma/keratinocyte heterocellular gap junctions.** REKs were co-cultured with WT BL6 cells or cells engineered to express Cx26-GFP or Cx43-GFP. Heterocellular cultures were double immunolabeled for Cx26 or Cx43 and E-cadherin or immunolabeled for E-cadherin only. In all cases, control or connexin-expressing BL6 cells did not exhibit clear evidence of Cx43 or Cx26 gap junction plaques at interfaces with E-cadherin-positive REKs even when examined under high magnification (*boxed insets*). *Asterisks* highlight some BL6 cells. *Inset* images were magnified 2×. *Bars*, 20 μm.

erate growth reduction observed in Cx43-expresing melanomas grown in monolayers. We hypothesize that contact-dependent signaling with keratinocytes and soluble factors produced by keratinocytes may act to further enhance the tumor suppression, similar to reported mechanisms proposed to control melanocyte growth and proliferation (8, 9, 50).

Because Cx43 reduced the malignant phenotype of melanomas *in vitro* and further in the context of keratinocytes, we sought to assess the tumorigenicity of connexin-expressing melanomas *in vivo*. The chick CAM avian embryo model has been widely used as a model for tumorigenesis *in vivo*, including the assessment of melanoma tumor growth and metastasis (26, 31). We found that control melanomas produced relatively large tumors, not unlike tumors produced by Cx26-expressing melanomas. Conversely, Cx43-expressing melanomas produced significantly smaller tumors. In our *in vitro* studies, Cx43-expressing melanomas displayed a 2.5-fold reduction in total cell number. Comparatively, these cells produced 4.5-fold smaller tumors *in vivo*, suggesting again that the tumor-suppressive effects of Cx43 are microenvironment-dependent, similar to our mixed culture studies with keratinocytes. Interestingly, the epithelial cells of the CAM have been reported to express Cx43 (51), providing a compatible connexin microenvironment, although we have no evidence that heterocellular gap junctions form *in vivo*. Furthermore, we have shown that Cx43 can reduce angiogenesis in breast cancer in a three-dimensional microenvironment (16). It is possible that these and other factors present within the *in vivo* microenvironment produce additive effects that reduce primary tumor size above the observed proliferative differences *in vitro*.

Collectively, these data show that Cx43 is a tumor suppressor in melanomas found within the relevant microenvironment of keratinocytes as well as *in vivo*. Additionally, we show that Cx26-based GJIC within melanomas does not result in tumor suppression, but rather, tumor suppression occurs because of

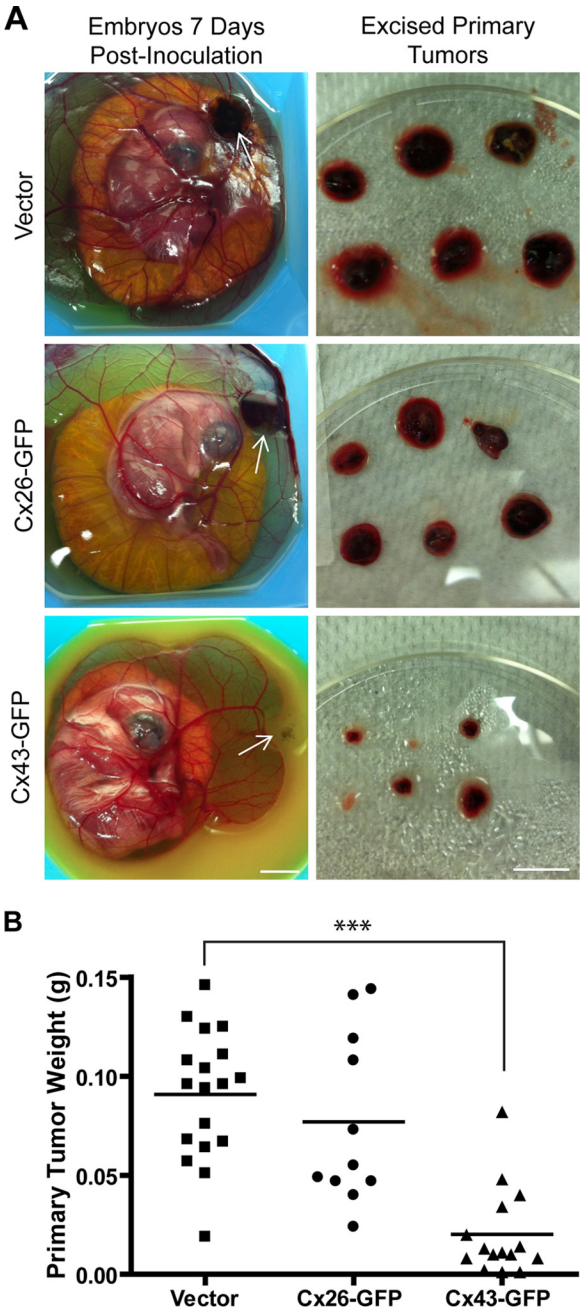

FIGURE 8. **Cx43 expression significantly reduces primary tumor growth *in vivo*.** *A*, 300,000 control or Cx-expressing melanomas were topically applied to the CAM of 10-day-old chicken embryos. Primary melanoma tumors visible on the CAM 7 days post-inoculation (*arrows*) were excised, photographed, and weighed. *B*, control melanomas produced large, blood-filled tumors of ~0.09 g in weight ($n = 18$). Cx26-GFP-expressing melanomas exhibited a slight reduction in primary tumor weight (~0.075 g), but this was not statistically significant ($n = 11$, p = ns). Conversely, melanomas expressing Cx43-GFP produced significantly smaller tumors of ~0.02 g in weight (~4.5-fold reduction from controls) ($n = 15$; ***, $p < 0.001$). *Bars*, 1 cm.

the specific expression of Cx43. The mechanism involved may be through the formation of Cx43-based gap junction channels or possibly through the less well understood Cx43-based hemichannels that allow selective communication between intra- and extracellular environments. This concept is not surprising when we consider the differences in molecules that are able to pass through each respective connexin-based channel. Not only are Cx43 channels capable of passing molecules excluded from Cx26 channels, but they also have different relative permeabilities to the same molecules (30). These differences in transjunctional molecules and molecular permeability properties undoubtedly lead to differences in gap junction-mediated cellular signaling and must be considered when evaluating the channel-dependent role of connexins during tumorigenesis. Additionally, Cx43 has been reported to interact with over 30 distinct proteins, compared with ~5 for Cx26 (46). In fact, several of these Cx43 binding partners have been implicated as tumor suppressors including caveolin-1 (52), CCN3 (53), TSG101 (54), and Src (55). Given this, as well as the many antiproliferative proteins that have been reported to be co-regulated with Cx43, the tumor-suppressive properties of Cx43 are likely specific to the cancer type and complex, involving both GJIC-dependent and independent mechanisms. Furthermore, although we did not re-establish GJIC between melanomas and keratinocytes in an attempt to mimic GJIC between melanocytes and keratinocytes as part of normal skin homeostasis (6), we show that increasing Cx43 expression and GJIC within melanomas has tumor-suppressive properties that are further enhanced in the presence of keratinocytes or other *in vivo*-like environments. Thus, Cx43 may prove to be a useful target for future drug therapeutic where Cx43 is selectively enhanced in melanomas.

REFERENCES

1. Söhl, G., and Willecke, K. (2003) An update on connexin genes and their nomenclature in mouse and man. *Cell Commun. Adhes.* **10,** 173–180
2. Wang, N., De Bock, M., Decrock, E., Bol, M., Gadicherla, A., Vinken, M., Rogiers, V., Bukauskas, F. F., Bultynck, G., and Leybaert, L. (2013) Paracrine signaling through plasma membrane hemichannels. *Biochim. Biophys. Acta* **1828,** 35–50
3. Richard, G. (2000) Connexins. A connection with the skin. *Exp. Dermatol.* **9,** 77–96
4. Hsu, M., Andl, T., Li, G., Meinkoth, J. L., and Herlyn, M. (2000) Cadherin repertoire determines partner-specific gap junctional communication during melanoma progression. *J. Cell Sci.* **113,** 1535–1542
5. Masuda, M., Usami, S., Yamazaki, K., Takumi, Y., Shinkawa, H., Kurashima, K., Kunihiro, T., and Kanzaki, J. (2001) Connexin 26 distribution in gap junctions between melanocytes in the human vestibular dark cell area. *Anat. Rec.* **262,** 137–146
6. Haass, N. K., and Herlyn, M. (2005) Normal human melanocyte homeostasis as a paradigm for understanding melanoma. *J. Investig. Dermatol. Symp. Proc.* **10,** 153–163
7. Seiberg, M., Paine, C., Sharlow, E., Andrade-Gordon, P., Costanzo, M., Eisinger, M., and Shapiro, S. S. (2000) The protease-activated receptor 2 regulates pigmentation via keratinocyte-melanocyte interactions. *Exp. Cell Res.* **254,** 25–32
8. Shih, I. M., Elder, D. E., Hsu, M. Y., and Herlyn, M. (1994) Regulation of Mel-CAM/MUC18 expression on melanocytes of different stages of tumor progression by normal keratinocytes. *Am. J. Pathol.* **145,** 837–845
9. Valyi-Nagy, I. T., Hirka, G., Jensen, P. J., Shih, I. M., Juhasz, I., and Herlyn, M. (1993) Undifferentiated keratinocytes control growth, morphology, and antigen expression of normal melanocytes through cell-cell contact. *Lab. Invest.* **69,** 152–159
10. Loewenstein, W. R., and Kanno, Y. (1966) Intercellular communication and the control of tissue growth. Lack of communication between cancer cells. *Nature* **209,** 1248–1249
11. Krutovskikh, V., Mazzoleni, G., Mironov, N., Omori, Y., Aguelon, A. M., Mesnil, M., Berger, F., Partensky, C., and Yamasaki, H. (1994) Altered homologous and heterologous gap-junctional intercellular communication in primary human liver tumors associated with aberrant protein lo-

calization but not gene mutation of connexin 32. *Int. J. Cancer* **56,** 87–94
12. Yamaoka, K., Nouchi, T., Tazawa, J., Hiranuma, S., Marumo, F., and Sato, C. (1995) Expression of gap junction protein connexin 32 and E-cadherin in human hepatocellular carcinoma. *J. Hepatol.* **22,** 536–539
13. Mesnil, M., Crespin, S., Avanzo, J. L., and Zaidan-Dagli, M. L. (2005) Defective gap junctional intercellular communication in the carcinogenic process. *Biochim. Biophys. Acta* **1719,** 125–145
14. Cronier, L., Crespin, S., Strale, P. O., Defamie, N., and Mesnil, M. (2009) Gap junctions and cancer. New functions for an old story. *Antioxid. Redox. Signal* **11,** 323–338
15. Eghbali, B., Kessler, J. A., Reid, L. M., Roy, C., and Spray, D. C. (1991) Involvement of gap junctions in tumorigenesis. Transfection of tumor cells with connexin 32 cDNA retards growth *in vivo*. *Proc. Natl. Acad. Sci. U.S.A.* **88,** 10701–10705
16. McLachlan, E., Shao, Q., Wang, H. L., Langlois, S., and Laird, D. W. (2006) Connexins act as tumor suppressors in three-dimensional mammary cell organoids by regulating differentiation and angiogenesis. *Cancer Res.* **66,** 9886–9894
17. Zhu, D., Caveney, S., Kidder, G. M., and Naus, C. C. (1991) Transfection of C6 glioma cells with connexin 43 cDNA. Analysis of expression, intercellular coupling, and cell proliferation. *Proc. Natl. Acad. Sci. U.S.A.* **88,** 1883–1887
18. Hirschi, K. K., Xu, C. E., Tsukamoto, T., and Sager, R. (1996) Gap junction genes Cx26 and Cx43 individually suppress the cancer phenotype of human mammary carcinoma cells and restore differentiation potential. *Cell Growth Differ.* **7,** 861–870
19. Loewenstein, W. R., and Rose, B. (1992) The cell-cell channel in the control of growth. *Semin. Cell Biol.* **3,** 59–79
20. King, T. J., and Lampe, P. D. (2004) The gap junction protein connexin32 is a mouse lung tumor suppressor. *Cancer Res.* **64,** 7191–7196
21. Temme, A., Buchmann, A., Gabriel, H. D., Nelles, E., Schwarz, M., and Willecke, K. (1997) High incidence of spontaneous and chemically induced liver tumors in mice deficient for connexin32. *Curr. Biol.* **7,** 713–716
22. Naus, C. C., and Laird, D. W. (2010) Implications and challenges of connexin connections to cancer. *Nat. Rev. Cancer* **10,** 435–441
23. Ito, A., Katoh, F., Kataoka, T. R., Okada, M., Tsubota, N., Asada, H., Yoshikawa, K., Maeda, S., Kitamura, Y., Yamasaki, H., and Nojima, H. (2000) A role for heterologous gap junctions between melanoma and endothelial cells in metastasis. *J. Clin. Invest.* **105,** 1189–1197
24. Su, Y. A., Bittner, M. L., Chen, Y., Tao, L., Jiang, Y., Zhang, Y., Stephan, D. A., and Trent, J. M. (2000) Identification of tumor-suppressor genes using human melanoma cell lines UACC903, UACC903(+6), and SRS3 by comparison of expression profiles. *Mol. Carcinog.* **28,** 119–127
25. Bagnato, A., Rosanò, L., Spinella, F., Di Castro, V., Tecce, R., and Natali, P. G. (2004) Endothelin B receptor blockade inhibits dynamics of cell interactions and communications in melanoma cell progression. *Cancer Res.* **64,** 1436–1443
26. Stoletov, K., Strnadel, J., Zardouzian, E., Momiyama, M., Park, F. D., Kelber, J. A., Pizzo, D. P., Hoffman, R., VandenBerg, S. R., and Klemke, R. L. (2013) Role of connexins in metastatic breast cancer and melanoma brain colonization. *J. Cell Sci.* **126,** 904–913
27. Saito-Katsuragi, M., Asada, H., Niizeki, H., Katoh, F., Masuzawa, M., Tsutsumi, M., Kuniyasu, H., Ito, A., Nojima, H., and Miyagawa, S. (2007) Role for connexin 26 in metastasis of human malignant melanoma. Communication between melanoma and endothelial cells via connexin 26. *Cancer* **110,** 1162–1172
28. Hsu, M. Y., Meier, F. E., Nesbit, M., Hsu, J. Y., Van Belle, P., Elder, D. E., and Herlyn, M. (2000) E-cadherin expression in melanoma cells restores keratinocyte-mediated growth control and down-regulates expression of invasion-related adhesion receptors. *Am. J. Pathol.* **156,** 1515–1525
29. Qin, H., Shao, Q., Curtis, H., Galipeau, J., Belliveau, D. J., Wang, T., Alaoui-Jamali, M. A., and Laird, D. W. (2002) Retroviral delivery of connexin genes to human breast tumor cells inhibits *in vivo* tumor growth by a mechanism that is independent of significant gap junctional intercellular communication. *J. Biol. Chem.* **277,** 29132–29138
30. Harris, A. L. (2007) Connexin channel permeability to cytoplasmic molecules. *Prog. Biophys. Mol. Biol.* **94,** 120–143
31. Penuela, S., Gyenis, L., Ablack, A., Churko, J. M., Berger, A. C., Litchfield, D. W., Lewis, J. D., and Laird, D. W. (2012) Loss of pannexin 1 attenuates melanoma progression by reversion to a melanocytic phenotype. *J. Biol. Chem.* **287,** 29184–29193
32. Laird, D. W., Jordan, K., Thomas, T., Qin, H., Fistouris, P., and Shao, Q. (2001) Comparative analysis and application of fluorescent protein-tagged connexins. *Microsc. Res. Tech.* **52,** 263–272
33. Thomas, T., Jordan, K., Simek, J., Shao, Q., Jedeszko, C., Walton, P., and Laird, D. W. (2005) Mechanisms of Cx43 and Cx26 transport to the plasma membrane and gap junction regeneration. *J. Cell Sci.* **118,** 4451–4462
34. Kalra, J., Shao, Q., Qin, H., Thomas, T., Alaoui-Jamali, M. A., and Laird, D. W. (2006) Cx26 inhibits breast MDA-MB-435 cell tumorigenic properties by a gap junctional intercellular communication-independent mechanism. *Carcinogenesis* **27,** 2528–2537
35. Falk, M. M. (2000) Connexin-specific distribution within gap junctions revealed in living cells. *J. Cell Sci.* **113,** 4109–4120
36. Jordan, K., Solan, J. L., Dominguez, M., Sia, M., Hand, A., Lampe, P. D., and Laird, D. W. (1999) Trafficking, assembly, and function of a connexin43-green fluorescent protein chimera in live mammalian cells. *Mol. Biol. Cell* **10,** 2033–2050
37. Thomas, T., Telford, D., and Laird, D. W. (2004) Functional domain mapping and selective trans-dominant effects exhibited by Cx26 disease-causing mutations. *J. Biol. Chem.* **279,** 19157–19168
38. Weber, P. A., Chang, H. C., Spaeth, K. E., Nitsche, J. M., and Nicholson, B. J. (2004) The permeability of gap junction channels to probes of different size is dependent on connexin composition and permeant-pore affinities. *Biophys. J.* **87,** 958–973
39. Sato, H., Hagiwara, H., Ohde, Y., Senba, H., Virgona, N., and Yano, T. (2007) Regulation of renal cell carcinoma cell proliferation, invasion and metastasis by connexin 32 gene. *J. Membr. Biol.* **216,** 17–21
40. Huang, R. P., Fan, Y., Hossain, M. Z., Peng, A., Zeng, Z. L., and Boynton, A. L. (1998) Reversion of the neoplastic phenotype of human glioblastoma cells by connexin 43 (cx43). *Cancer Res.* **58,** 5089–5096
41. Ionta, M., Ferreira, R. A., Pfister, S. C., and Machado-Santelli, G. M. (2009) Exogenous Cx43 expression decrease cell proliferation rate in rat hepatocarcinoma cells independently of functional gap junction. *Cancer Cell Int.* **9,** 22
42. Princen, F., Robe, P., Gros, D., Jarry-Guichard, T., Gielen, J., Merville, M. P., and Bours, V. (2001) Rat gap junction connexin-30 inhibits proliferation of glioma cell lines. *Carcinogenesis* **22,** 507–513
43. Zhang, Y. W., Nakayama, K., Nakayama, K., and Morita, I. (2003) A novel route for connexin 43 to inhibit cell proliferation. Negative regulation of S-phase kinase-associated protein (Skp 2). *Cancer Res.* **63,** 1623–1630
44. Chen, S. C., Pelletier, D. B., Ao, P., and Boynton, A. L. (1995) Connexin43 reverses the phenotype of transformed cells and alters their expression of cyclin/cyclin-dependent kinases. *Cell Growth Differ.* **6,** 681–690
45. Omori, Y., and Yamasaki, H. (1999) Gap junction proteins connexin32 and connexin43 partially acquire growth-suppressive function in HeLa cells by deletion of their C-terminal tails. *Carcinogenesis* **20,** 1913–1918
46. Laird, D. W. (2010) The gap junction proteome and its relationship to disease. *Trends Cell Biol.* **20,** 92–101
47. Zucker, S. N., Bancroft, T. A., Place, D. E., Des Soye, B., Bagati, A., and Berezney, R. (2013) A dominant negative Cx43 mutant differentially affects tumorigenic and invasive properties in human metastatic melanoma cells. *J. Cell Physiol.* **228,** 853–859
48. Elzarrad, M. K., Haroon, A., Willecke, K., Dobrowolski, R., Gillespie, M. N., and Al-Mehdi, A. B. (2008) Connexin-43 upregulation in micrometastases and tumor vasculature and its role in tumor cell attachment to pulmonary endothelium. *BMC Med.* **6,** 20
49. Pollmann, M. A., Shao, Q., Laird, D. W., and Sandig, M. (2005) Connexin 43 mediated gap junctional communication enhances breast tumor cell diapedesis in culture. *Breast Cancer Res.* **7,** R522–534
50. Haass, N. K., Smalley, K. S., and Herlyn, M. (2004) The role of altered cell-cell communication in melanoma progression. *J. Mol. Histol.* **35,** 309–318
51. Girolamo, F., Elia, G., Errede, M., Virgintino, D., Cantatore, S., Lorusso, L., Roncali, L., Bertossi, M., and Ambrosi, L. (2006) *In vivo* assessment of

epichlorohydrin effects. The chorioallantoic membrane model. *Med. Sci. Monit.* **12,** BR21–BR27

52. Langlois, S., Cowan, K. N., Shao, Q., Cowan, B. J., and Laird, D. W. (2010) The tumor-suppressive function of Connexin43 in keratinocytes is mediated in part via interaction with caveolin-1. *Cancer Res.* **70,** 4222–4232
53. Fu, C. T., Bechberger, J. F., Ozog, M. A., Perbal, B., and Naus, C. C. (2004) CCN3 (NOV) interacts with connexin43 in C6 glioma cells. Possible mechanism of connexin-mediated growth suppression. *J. Biol. Chem.* **279,** 36943–36950
54. Leithe, E., Kjenseth, A., Sirnes, S., Stenmark, H., Brech, A., and Rivedal, E. (2009) Ubiquitylation of the gap junction protein connexin-43 signals its trafficking from early endosomes to lysosomes in a process mediated by Hrs and Tsg101. *J. Cell Sci.* **122,** 3883–3893
55. Kieken, F., Mutsaers, N., Dolmatova, E., Virgil, K., Wit, A. L., Kellezi, A., Hirst-Jensen, B. J., Duffy, H. S., and Sorgen, P. L. (2009) Structural and molecular mechanisms of gap junction remodeling in epicardial border zone myocytes following myocardial infarction. *Circ. Res.* **104,** 1103–1112